Published in final edited form as:
Bioconjug Chem. 2009 May 20; 20(5): 937–943. doi:10.1021/bc800520d.

Comparison of synthetic HDL contrast agents for MR imaging of atherosclerosis

David P. Cormode[1], **Rohith Chandrasekar**[2], **Amanda Delshad**[1], **Karen C. Briley-Saebo**[1], **Claudia Calcagno**[1], **Alessandra Barazza**[1,3], **Willem J. M. Mulder**[1], **Edward A. Fisher**[3], and **Zahi A. Fayad**[1]

[(1)]Translational and Molecular Imaging Institute, Mount Sinai School of Medicine, One Gustave L. Levy Place, Box 1234, New York, NY 10029, Tel: 212-241-6858, Fax: 240-368-8096, Zahi.Fayad@mssm.edu

[(2)]The Cooper Union for the Advancement in Science and Art, 30 Cooper Square, New York, NY 10003

[(3)]Department of Medicine (Cardiology), Marc and Ruti Bell Vascular Biology and Disease Program and the NYU Center for the Prevention of Cardiovascular Disease, New York University School of Medicine, New York University, Smilow 8 522 First Ave., New York, NY 10016, Tel: 212-263-6636, Fax: 212-263-6632 Edward.Fisher@nyumc.org

Abstract

Determining arterial macrophage expression is an important goal in the molecular imaging of atherosclerosis. Here we compare the efficacy of two synthetic, HDL-based contrast agents for magnetic resonance imaging (MRI) of macrophage burden. Each form of HDL was labeled with gadolinium and rhodamine to allow MRI and fluorescence microscopy. Either the 37 or 18 amino acid peptide replaced the apolipoprotein A-I in these agents, which were termed 37pA-Gd or 18A-Gd. The diameters of 37pA-Gd and 18A-Gd are 7.6 nm and 8.0 nm, respectively, while the longitudinal relaxivities are 9.8 and 10.0 $(mMs)^{-1}$. 37pA has better lipid binding properties. *In vitro* tests with J774A.1 macrophages proved the particles possessed the functionality of HDL by eliciting cholesterol efflux and were taken up in a receptor-like fashion by the cells. Both agents produced enhancements in atherosclerotic plaques of apolipoprotein E knockout mice of ~90% (n=7 per agent) and are macrophage specific as evidenced by confocal microscopy on aortic sections. The half-lives of 37pA-Gd and 18A-Gd are 2.6 and 2.1 hours, respectively. Despite the more favorable lipid interactions of 37pA, both agents gave similar, excellent contrast for the detection of atherosclerotic macrophages using MRI.

Keywords

atherosclerosis; lipoproteins; macrophages; MRI

Correspondence to: Edward A. Fisher; Zahi A. Fayad.

Supporting Information Available The method for macrophage efflux determination and further details of the MRI scanning setup can be found online. Furthermore, figures displaying the uptake of 18A-Gd and 37pA-Gd in macrophages as a function of time (S1 and S2), the uptake of Gd-micelles in macrophages as a function of concentration (S3) and a confocal microscopy image of the aorta of an apoE mouse where there are no macrophages (S4) are included in the supporting information. This material is available free of charge via the Internet at http://pubs.acs.org/.

Main Text

Heart disease is now the primary cause of mortality in the world (1). The most common factor behind adverse cardiovascular events is rupture of vulnerable plaques caused by atherosclerosis (2). As such there is a significant motivation to image atherosclerotic tissue for diagnosis, to characterize disease stage, and to monitor the effect of therapy (3,4). One of the favored courses of action is to non-invasively image atherosclerotic plaques using magnetic resonance imaging (MRI) (5,6), since this imaging modality has high spatial resolution, excellent soft tissue contrast and does not expose the patient to ionizing radiation. While MRI without contrast can determine plaque morphology and some features of plaque composition, targeted contrast agents are required to fully determine the cellular composition of the plaque.

Macrophages are key in the progression of atherosclerosis, entering the intima as monocytes, being activated to macrophages via interaction with and uptake of modified low density lipoprotein, until they become foam cells and eventually forming the necrotic lipid core associated with unstable plaques (7). Furthermore, macrophage content has been identified as a key biological marker of vulnerable plaques. As a result, several methods have been proposed for molecular imaging of these cells in diseased arteries, for example using targeted, gadolinium-labeled micelles (8,9) or dextran coated iron oxides (10) for MRI, iodine nanoparticles for computed tomography (11) or ^{18}F-2-fluoro-2-deoxyglucose and ^{64}Cu labeled nanoparticles with positron emission tomography (12,13). We have previously reported the use of gadolinium (Gd^{3+}) and fluorophore modified high density lipoprotein (HDL), an endogenous nanoparticle naturally targeted to atherosclerotic plaques, to image macrophage burden in the abdominal aorta of a mouse model of atherosclerosis (14,15). A restriction to the translation of this methodology to the clinic is the absence of a ready commercial source of apo A-I. Therefore we recently reported preliminary data on a synthetic, MRI-active HDL formulation based on the amphiphatic peptide 37pA and gadolinium labeled phospholipids (16). 37pA, which mimics the properties of the major protein component of HDL, apoA-I (18), is composed of 37 amino acid residues and binds to lipidic particles strongly (19).

We report here the synthesis of an MRI-active HDL-based contrast agent formed using 18A, another apoA-I mimicking peptide composed of only 18 amino acid (20) residues and an extensive comparison of this and the 37pA-based agent. The advantage of 18A over 37pA is that this shorter peptide is easier and less expensive to synthesize ($1584 for 18A vs $3541 for 37pA, both figures are for 100 mg, 95% purity, Global Peptide Services). The lipid binding properties of 18A, however, are inferior to 37pA, the peptides having an egg phosphatidylcholine exclusion pressure of 30 dyn/cm and 41 dyn/cm, respectively (19). The superior lipid binding properties of 37pA may result in a better MR enhancement of the arterial wall since the gadolinium-labeled phospholipids in the HDL mimetic are held together more strongly and may be delivered to the atherosclerotic plaque with greater efficiency. Nevertheless, it is unclear if this would affect the efficacy of the agents for *in vivo* MR imaging studies. In this report we compare the 18A-based agent with the 37pA-based agent by investigating their physical properties, *in vitro* macrophage efflux, *in vitro* macrophage uptake, and MR imaging efficacy in apolipoprotein E knockout (apoE-KO) mice. In addition, the biodistribution and pharmacokinetics of the agents were assessed. As will be shown, despite theoretical advantages of 37pA, comparable imaging efficacies were obtained with the 18A peptide.

Experimental Procedures

Materials

Dimyristoyl phosphatidylcholine (DMPC), gadolinium 1,2-dimyristoyl-sn-glycero-3-phosphoethanolamine diethylenetriamine pentaacetic acid (Gd-DTPA-DMPE) and 1,2-

dimyristoyl-sn-glycero-3-phosphoethanolamine-N-(lissamine rhodamine B sulfonyl) ammonium salt (Rhod-PE) were all purchased from Avanti Polar Lipids and used as received. Cy5.5-labeled dimyristoyl phosphoethanolamine (Cy5.5-PE) was synthesized as described below. The peptides 18A (sequence: DWL KAF YDK VAE KLK EAF) and 37pA (sequence: DWL KAF YDK VAE KLK EAF PDW LKA FYD KVA EKL KEA F) were synthesized by Global Peptide Services (Fort Collins, CO) at 95% purity. Cell culture supplies were purchased from Invitrogen (Carlsbad, CA).

Nanodisc synthesis

To form synthetic, MRI-active HDL using 18A, a 200:200:1 mixture by mass of DMPC, Gd-DTPA-DMPE and Rhod-PE (25 mg) were dissolved in a 1:4 mixture of methanol and chloroform. A lipid film was formed under vacuum from this solution, which was hydrated with a solution of 18A in 5ml of 1× PBS such that there was 1 mg of peptide, for each 2.5 mg of phospholipids used. The resulting mixture was heated at 65 °C for 45 min, before being sonicated for 30 min on ice to form nano-discs, which were purified via centrifugation, filtration and washing. This product was termed 18A-Gd and was characterized by dynamic light scattering (DLS), gel permeation, gel electrophoresis, relaxometry, gadolinium quantification, protein analysis and phosphate quantification. Details of the characterization methodology may be found in reference (16). 37pA-Gd and Gd-micelles (micelles forming using the same phospholipid mixture as for 18A-Gd and 37pA-Gd but without any peptide) were synthesized as previously described (16). A schematic depiction of 18A-Gd and 37pA-Gd is displayed in Figure 1. The disk-like structure of such phospholipid-peptide aggregates has been established by ourselves (16) and others (17).

Cy5.5-PE Synthesis

For incorporation in the synthetic HDL nanoparticles, Cy5.5 mono reactive NHS esters were conjugated to dimyristoyl phosphoethanolamine (DMPE). Typically, 50 μmol DMPE and 50 μmol stearoyl-hydroxy phosphatidylcholine (SHPC) was dissolved in 3 ml of a 4:1 chloroform: methanol solvent mixture. The solvents were removed from this solution to form a lipid film, which was subsequently hydrated for 30 minutes via agitation with 5 ml of a 0.1 M sodium bicarbonate aqueous solution (pH ~8.4) at room temperature to form micelles. After this 20 mg Cy5.5 mono NHS ester was dissolved in 250 μl DMSO, which was added to the DMPE-SHPC micelle aqueous solution. The mixture was stirred overnight at 4 °C under nitrogen atmosphere to allow for the conjugation of Cy5.5 to the lipids. A 50 kDa Vivaspin molecular weight cut-off tube was used to separate unconjugated Cy5.5 mono NHS ester from Cy5.5 conjugated lipid micelles, by washing 10 times with water until the residue was completely colorless. The Cy5.5 micelles were subsequently freeze dried for 3 days to remove all water, after which they were dissolved in a 20:1 chloroform:methanol mixture.

Macrophage uptake of reconstituted HDL

J774A.1 murine macrophage cells were cultured in DMEM supplemented with 10% FBS and 1% streptomycin/penicillin. The cells were passaged 5 times before the incubations took place. The cells were grown to 70-80% confluency, before being plated in black, non-fluorescent 96 wells plates the day prior to incubation. For these studies agents labeled with Cy5.5-PE instead of Rhod-PE were used. 18A-Gd or 37pA-Gd was added to one row (12 wells) for each condition, with untreated cells and wells incubated with media only or Gd-micelles as controls. The cells were incubated at a concentration of 0.02 mM Gd at time points from 1 to 24 hours. Further experiments were carried out where the incubation time was held constant at 2 hours and the concentration of the agent varied from 0.01 to 0.16 mM Gd. Incubations were performed where the agent uptake at 0.02 mM and 2 hours was compared with macrophages also incubated with a tenfold excess (by protein content) of non-Cy5.5 labeled 18A-Gd or

37pA-Gd. Last, the agent uptake of macrophages and smooth muscle cells (derived from Wistar rats, see supporting information for more detail) was compared. After incubation, the media was removed, the cells were washed with cold (4°C) PBS three times and fixed with 4% paraformaldehyde. The cells were imaged in the plates using an IVIS Imaging System 200 (Xenogen, Alameda, CA). The plates were illuminated for 5 s using a 150 W Quartz halogen lamp filtered by the 615-665 nm Cy5.5 excitation band, while the emission was quantitatively recorded using the 695-770 nm Cy5.5 emission filter. Images were analyzed and the fluorescence from each well was determined using the software supplied with the IVIS system.

Smooth muscle cell isolation and culture

Rat airway smooth muscle (ASM) cells were isolated from 10 week old male Wistar rats. Rats were intra-peritoneally injected with pentobarbital sodium (35mg/kg), and the tracheas were aseptically excised and placed in Ca^{2+}, Mg^{2+} -free Hanks balanced salt solution (HBSS) (SIGMA). The isolated tracheas were cleaned of connective tissues, cut longitudinally through the cartilage, and enzymatically dissociated with filtered HBSS containing 0.2% collagenase type 2 (Worthington Biochemical Corporation, Lakewood, NJ) for 30mins in a shaking waterbath at 37°C. Dissociated cells in suspension were centrifuged and resuspended in Dulbecco's modified Eagle's medium (DMEM)-Ham's F12 medium (1:1 vol/vol) (SIGMA) supplemented with 10% FCS (GIBCO) and (100 U/ml penicillin, 100μg/ml streptomyocin (GIBCO). Cells were plated on petri dishes and grown until confluence at 37°C in humidified air containing 5% CO_2. The medium was changed every 48hrs and confluent cells were passaged with 0.25%-0.02% EDTA solution (GIBCO). ASM cells in culture were elongated and spindle shaped, grew with typical hill and valley appearance, and stained positively for the smooth muscle specific protein α-actin. Cells were used at the second passage.

Animal model of atherosclerosis

Both apoE-KO and wild type mice were used in this study. The apoE-KO mice were an average of 10 months old and fed a high cholesterol diet to induce plaque development for an average of 8 months prior to use in these experiments. The wild type mice were fed an ordinary chow diet and were the same average age. All mice were male and were housed and maintained at the Mount Sinai Animal Facility. The Mount Sinai School of Medicine Institute of Animal Care and Use Committee approved all experiments.

In vivo MR imaging

In vivo MRI was performed using a 9.4 T, 89 mm bore MRI system (Bruker Instruments, Billerica, MA). The imaging system and methodology are extensively described in reference (8). After a preinjection baseline MRI scan, mice were injected, via a tail-vein catheter. Subsequent scans were carried out at 24, 48, 72 and 96 hours post-injection. n=7 apoE-KO mice and n=2 wild type mice were injected with 18A-Gd, the same group sizes used in the previous 37pA study. Use of the medical image analysis software package eFilm allowed the MR signal intensity of various tissues from the different time points to be ascertained and the percent change in normalized enhancement ratio (% NER) post-injection to be calculated. Normalization of the MR signal intensity in the aorta wall was performed by rebasing with the signal from the adjacent muscle to create the value W. The % NER was found from the difference between W from the post-injection scans and W from the pre-scan divided by W from the prescan and multiplied by 100, as per the method described in (8).

Confocal microscopy

ApoE-KO mice were sacrificed 24 hours after injection with contrast agent. The mice were perfused with saline at physiological pressure and their aortas removed. 3 mm pieces of the aorta were embedded in Tissue-Tek Optimal Cutting Temperature media (Sakura Finetek,

Torrance, CA), frozen, sectioned and fixed in paraformaldehyde. These sections of aorta were stained with Alexa 647-CD68, a macrophage specific antibody conjugated to a fluorophore before the section was fixed in a DAPI (nuclei specific) containing agent and coverslipped. Confocal laser scanning microscopy on aortic sections was performed using a Zeiss LSM 510 META microscope (Carl Zeiss, Oberkochen, Germany) in an inverted configuration. Colocalization of rhodamine (contrast agent) and CD68 staining (macrophages) in the confocal microscopy images was quantified using an in-house developed image analysis software tool based in MatLab R2007b (Natick, MA).

Pharmacokinetics and Biodistribution

To determine the pharmacokinetics of 37pA-Gd, 18A-Gd and Gd-micelles, a 50 μmol/kg dose of the agent was injected into apoE-KO mice whose hair on their lower limbs had been removed to allow access to the saphenous veins. Blood (10-20 μl) was drawn from these veins at 5 min, 30 min, 1 hour, 2 hours, 3 hours, 4 hours, 24 hours and 48 hours post injection and placed into pre-weighed vials containing 80 μl of heparin. The vials were weighed again to determine the volume of blood drawn, the density of blood being taken to be 1.05 g/ml (21). The gadolinium content of the blood for each timepoint was determined by inductively coupled plasma mass spectrometry (ICP-MS) performed on the blood-heparin mixture and adjusting for the blood volume. Half-lives were calculated from analysis of the variance of blood gadolinium content over time with the MatLab software package using a biexponential model.

The biodistribution was determined for 37pA-Gd and 18A-Gd at 48 hours after injection of the agents into apoE-KO mice at a 50 μmol/kg dose. The animals were sacrificed by perfusion with saline administered via the left ventricle of the heart. The liver, kidneys, heart, spleen and lungs were removed, weighed and homogenized before analysis via ICP-MS for determination of Gd content. The per unit weight gadolinium content thus found was multiplied by the organ wet weight and divided by the injected dose to give the biodistribution. Cantest Ltd (Burnaby, Canada) performed all ICP-MS analyses.

Statistical analysis

Data populations were compared using Student's t-test (two-tailed, heteroscedastic). Populations were considered to be significantly different if $p<0.01$.

Results

Characterization

The average diameter of the 18-Gd particles was found via DLS to be 8.0 ± 0.3 nm. Using gel electrophoresis, the size was found to be approximately 7.6 nm. The corresponding values for the 37pA-Gd complex are very similar, being 7.6 nm by both techniques. FPLC gave only one peak in a narrow size distribution, indicating high product purity. The longitudinal relaxivity was found to be 10.0 ± 0.2 $mM^{-1}s^{-1}$, which is not significantly different from relaxivities reported for previous HDL-based contrast agents that used the same gadolinium chelating phospholipid (14,16). The gadolinium, phosphorous and protein analyses gave a relative mass ratio of Gd-DTPA-DMPE:DMPC:18A of 1.18:1.10:1, which deviates somewhat from the input values of 1.25:1.25:1 and indicates a less efficient particle formation than for the 37pA-Gd agent (whose values were 1.23:1.23:1). This may be due to the lower lipid binding parameters of 18A as compared to the dual domain peptide 37pA (19).

Macrophage Cholesterol Efflux

HDL-based particles have therapeutic properties in terms of their anti-inflammatory action as well as their ability to retrieve cholesterol from atherosclerotic plaques and transport it to the

liver for excretion (7). A common measure of this latter property is macrophage cholesterol efflux, i.e. the quantity of cholesterol removed from macrophages by an agent (22). We performed such experiments using 18A-Gd and 37pA-Gd, while native HDL (CSL Behring, Bern, Switzerland) was used as a comparison and bovine serum albumin (BSA) was used as a control (phospholipid-only species are well established to give substantially lower macrophage cholesterol efflux than synthetic HDL nanoparticles (22)). Each agent was used with the same concentration of peptide/protein. The efflux produced by HDL after 4 hours was 8.15 ± 0.27% of the total, for 18A-Gd 12.82 ± 0.29%, for 37pA-Gd 9.89 ± 0.20% and for BSA 1.61 ± 0.19%. Thus HDL, 18A-Gd and 37pA-Gd produce significantly more cholesterol efflux than the control, BSA. Both 18A-Gd and 37pA-Gd removed more cholesterol than the native HDL used, which is unsurprising as the HDL used in this study was more highly lipidated than the peptide-based nanoparticle, and so can accept a lesser amount of cholesterol from the macrophages. That this 18A complex produces a greater level of efflux than the 37pA complex is consistent with the results of investigations carried out by Davidson et al (22).

Macrophage uptake of 18A-Gd and 37pA-Gd

To investigate *in vitro* effectiveness of 18A-Gd and 37pA-Gd and whether uptake was a receptor-like specific process, we performed extensive incubations of Cy5.5-labeled formulations of the agents with murine macrophages. Plates of incubated cells were analyzed using a fluorescence imaging system, resulting in images such as those shown in Figure 2A. We found that uptake increased over time until 4 hours, after which increases in uptake were insubstantial (see supporting information, Figures S1 and S2), suggesting a saturable process. Cy5.5 was used in these experiments due to the lower adsorption of light by biological components in the wavelengths in which this fluorophore emits compared to Rhodamine, allowing better quantification of particle uptake (23). Macrophages incubated under competition-inhibition conditions (i.e. with a ten-fold excess of unlabeled agent in addition to the labeled agent) exhibited significantly less fluorescence than macrophages incubated with labeled agent only (Figure 2B), suggesting specificity. Furthermore, smooth muscle cells incubated with the agents took up significantly less agent than macrophages incubated under the same conditions (Figure 2C). Lastly, when macrophages were incubated with 18A-Gd and 37pA-Gd at concentrations ranging from 0.01 to 0.16 mM Gd, the uptake increased only slightly when the concentration increased from 0.04 mM to 0.16 mM Gd (Figures 2D and E), again suggesting a saturable process. Taken together, these data strongly indicate that the uptake of these synthetic HDL particles is specific, saturable process that is receptor-like in its characteristics. This would be compatible with interactions with HDL-interacting membrane proteins highly expressed by macrophages. The uptake of 18A-Gd and 37pAGd was not found to differ significantly. In comparison, macrophages took up Gdmicelles to a much lesser extent that for 18A-Gd or 37pA-Gd, in the concentration range 0.01 mM Gd to 0.16 mM Gd (Figure 2A and B, Figure S3). Furthermore, the uptake was linear, indicating uptake through an aspecific pathway and confirming the need for the peptides to produce a macrophage specific agent.

In vivo MR imaging

Representative images of the aorta of an apoE-KO mouse pre- and 24 hours post-injection with 18A-Gd are displayed in Figure 3A (left panels, the enhanced structure below the aorta in the post-image for 18A-Gd is a lymph node, which typically accumulate injected nanoparticles substantially). Visual inspection of the images indicates that there is significant enhancement of the image intensity in the aorta post-injection with 18A-Gd and that the enhancement is comparable to that observed post-injection with 37pA-Gd (Figure 3A, right panels). The results of analysis of the images from 7 mice for each agent imaged pre- and 24, 48, 72 and 96 hours post-injection with each agent are displayed in Figure 3B.

18A-Gd gives an average enhancement in the aorta wall of 91% at 24 hours, before declining steadily to 17% at 96 hours. Application of this agent to wild type mice gave only insignificant enhancements (< 8%, data not shown) in the aorta wall. Injection of Gd-micelles (composed of the same phospholipids as 18A-Gd and 37pA but without any peptide) into apoE-KO mice gave a maximum of 16% enhancement, which occurred at 24 hours. This value was significantly less than that of 18A-Gd and 37pA-Gd, showing the importance of the peptides for targeting the particles to atherosclerosis. The enhancement for 37pA-Gd at the 24 hour timepoint was slightly higher at 94%, but upon comparison of the data for 18A-Gd and 37pA-Gd using Student's t-test, the difference in the average enhancement at this timepoint was not found to be significant. In addition, the differences were not significant at 48 or 96 hours, however for the 72 hour timepoint the difference in the average enhancement produced by the two agents was found to be significant at the 1% level.

Confocal Microscopy

A typical confocal microscopy image of an aorta section excised from an apoE-KO mouse injected 24 hours previously with 18A-Gd is displayed in Figure 4. As can be seen there is a high level of rhodamine (red) signal in the plaque, in agreement with the MR imaging data that indicated plaque enhancement. The rhodamine co-localizes extensively with the macrophage staining (green), resulting in patches of yellow color in the merged image, indicative of macrophage specificity. Analysis of the confocal microscopy image using an in-house developed software tool revealed that 93% of the rhodamine signal co-localizes with CD68 positive regions, confirming the visual impression of macrophage specificity. In sections of the aorta that did not bear atherosclerotic plaques no rhodamine signal could be observed (see Supporting Information, Figure S4).

Pharmacokinetics and biodistribution

The pharmacokinetics of 18-Gd, 37pA-Gd and Gd-micelles were determined by analysis of blood drawn sequentially from mice injected with the agents. The half-life of 18A-Gd was found to be 2.1 +/- 0.1 hours, 2.6 +/- 0.3 hours for 37pA-Gd and 2.4 +/- 0.3 hours for Gd-micelles, with no significant difference between them, meaning the agents can be directly compared. The biodistributions of 18A-Gd and 37pA-Gd at 48 hours are displayed in Figure 5, given as the percentage of the injected dose. As can be seen, the vast majority of the retained dose is in the liver, with only a minor quantity in the spleen and negligible amounts in the lungs and heart. The levels of agent found in the kidneys are high compared to many contrast agents, but HDL is known to interact with these organs (24). The differences in biodistribution between the two agents are not statistically significant.

Discussion

In this report, we compared the physical properties, *in vitro* macrophage interactions and *in vivo* imaging efficacy of two different HDL-based MRI agents. Both contained apoA-I mimicking peptides, one being 37pA, the other 18A. The physical properties of the two agents are very similar, excepting a superior efficiency of lipid binding in the case of 37pA-Gd. In terms of the *in vitro* properties, 18A-Gd appears to have a slight advantage. Macrophage efflux measurements show 18A-Gd to interact with these cells to a greater extent than 37pA-Gd, which is in agreement with previous studies by Davidson et al (22). It could be the case that poor lipid binding properties are advantageous for interactions with macrophages, at least in the case of efflux, giving the particle the flexibility to distort to accept cholesterol. We have shown the agents 18A-Gd and 37pA-Gd to have receptor-like mediated uptake *in vitro*. 18A and 37pA have both been shown by others to bind to proteins highly expressed on macrophage cells (18,24), while we have recently shown HDL particles whose core is modified to contain gold, iron oxide or quantum dot nanoparticles to be internalized into macrophage cells (25).

Taken together, the evidence suggests that membrane proteins highly expressed on macrophages allow the specific uptake of 18A-Gd and 37pA-Gd observed *in vivo* as part of a receptor-mediated endocytic process.

The *in vivo* imaging properties of the two contrast agents are not significantly different, both giving excellent enhancement in atherosclerotic plaque of apoE-KO mice at 24 hours post-injection, as compared to pre-contrast imaging. Immunofluorescence performed upon excised aortas of mice injected with 18A-Gd gave a similar level of co-localization with macrophages as 37pA-Gd. The pharmacokinetics of the agents are interesting as they are relatively short and correspond more to those observed for micellar agents (26) than for lipoproteins ($t_{½}$ = 6 hours) (27). This could be due to enhanced rate of clearance due to the negative charge of the particles (28) (the gadolinium lipids have an overall negative charge). For studies of this sort, it is preferable to acquire post-injection images at timepoints at least five times the half-life of the contrast agent. As the half-life of the agents was around 2.5 hours, it might be that better contrast in the aorta could occur in scans acquired at 12.5 hours post-injection. In terms of biodistribution, both agents have very similar properties.

While increases in signal were observed in the aorta wall upon administration of the synthetic HDL agents, it is important to note that hyperintense areas were found, such as in the top left for both 18A-Gd and 37pA-Gd in Figure 3A. Additionally, there were sections of the aorta in both the animals depicted in this figure that bore atherosclerotic plaques, but the increase in signal was very small. As these agents are macrophage specific, this suggests that the hyperintense plaques are macrophage-rich and thus bear hallmarks of vulnerable plaques.

Molecular imaging of cardiovascular disease is critical for the early detection and monitoring of atherosclerosis. In the current study we present a low cost and potentially translatable agent for the in vivo MR imaging of intra-plaque macrophages. Other groups have proposed iron oxide based MR agents, which are desirable from both a safety (liver cells safely excrete iron) and efficacy (strong T2* effects) point of view. However, clinical studies using Sinerem/Combidex (Guerbet, France) reveal that this ultrasmall iron oxide particle must be administered as an infusion to both increase efficacy and reduce toxic effects. Additionally, but importantly, there are some serious limitations to imaging negative contrast caused by iron oxide in the vessel wall (29). Therefore we feel that our agent may offer some significant advantages over the alternatives that have been proposed. In addition, agents based on such peptides may be re-routed to other molecular targets (30), so this platform is not limited to macrophage imaging.

In summary, the HDL-based, MRI-active contrast agents 18A-Gd and 37pA-Gd have been extensively investigated as to their physical properties, *in vitro* macrophage interactions, potential as *in vivo* molecular imaging agents for macrophages in atherosclerosis and their excretion. The two agents have similar effectiveness with respect to *in vivo* imaging, however the 18A particles exhibit better cholesterol efflux. Based on these findings and due to the fact that the smaller 18A peptide is less expensive to manufacture we recommend the 18A peptide be used for future investigations. We plan to continue to investigate 18A-Gd via testing in rabbit models of atherosclerosis using clinical scanners and to create new molecular imaging contrast agents based on this peptide.

Supplementary Material

Refer to Web version on PubMed Central for supplementary material.

Acknowledgements

We gratefully acknowledge Dr. Gustav Strijkers of the Eindhoven University of Technology for assisting with the MRI sequences. We thank Daniel Samber of Mount Sinai School of Medicine for developing the confocal image

analysis software tool. We thank Joanne Stocks of Mount Sinai School of Medicine for providing the smooth muscle cells. We thank CSL Behring, Bern, Switzerland for their kind gift of reconstituted HDL.

Sources of Funding Partial support was provided by: NIH/NHLBI ROI HL71021, NIH/ NHLBI HL78667 (ZAF, EAF). Confocal microscopy was performed at the MSSM-Microscopy Shared Resource Facility and supported by NIH-National Cancer Institute Grant 5R24 CA095823-04, National Science Foundation Grant DBI-9724504, and NIH Grant 1 S10 RR0 9145-01.

References

(1). Fuster V, Voute J, Hunn M, Smith SC. Low priority of cardiovascular and chronic diseases on the global health agenda: a cause for concern. Circulation 2007;116:1966–1970. [PubMed: 17965407]

(2). Naghavi M, Libby P, Falk E, Casscells SW, Litovsky S, Rumberger J, Badimon JJ, Stefanadis C, Moreno P, Pasterkamp G, Fayad Z, Stone PH, Waxman S, Raggi P, Madjid M, Zarrabi A, Burke A, Yuan C, Fitzgerald PJ, Siscovick DS, de Korte CL, Aikawa M, Airaksinen KEJ, Assmann G, Becker CR, Chesebro JH, Farb A, Galis ZS, Jackson C, Jang IK, Koenig W, Lodder RA, March K, Demirovic J, Navab M, Priori SG, Rekhter MD, Bahr R, Grundy SM, Mehran R, Colombo A, Boerwinkle E, Ballantyne C, Insull W, Schwartz RS, Vogel R, Serruys PW, Hansson GK, Faxon DP, Kaul S, Drexler H, Greenland P, Muller JE, Virmani R, Ridker PM, Zipes DP, Shah PK, Willerson JT. From vulnerable plaque to vulnerable patient - A call for new definitions and risk assessment strategies: Part I. Circulation 2003;108:1664–1672. [PubMed: 14530185]

(3). Choudhury RP, Fuster V, Fayad ZA. Molecular, cellular and functional imaging of atherothrombosis. Nat. Rev. Drug Discov 2004;3:913–925. [PubMed: 15520814]

(4). Sanz J, Fayad ZA. Imaging of atherosclerotic cardiovascular disease. Nature 2008;451:953–957. [PubMed: 18288186]

(5). Jaffer FA, Libby P, Weissleder R. Molecular imaging of cardiovascular disease. Circulation 2007;116:1052–1061. [PubMed: 17724271]

(6). Leiner T, Gerretsen S, Botnar R, Lutgens E, Cappendijk V, Kooi E, van Engelshoven J. Magnetic resonance imaging of atherosclerosis. Eur. Radiol 2005;15:1087–1099. [PubMed: 15723215]

(7). Lusis AJ. Atherosclerosis. Nature 2000;407:233–241. [PubMed: 11001066]

(8). Amirbekian V, Lipinski MJ, Briley-Saebo KC, Amirbekian S, Aguinaldo JG, Weinreb DB, Vucic E, Frias JC, Hyafil F, Mani V, Fisher EA, Fayad ZA. Detecting and assessing macrophages in vivo to evaluate atherosclerosis noninvasively using molecular MRI. Proc. Natl. Acad. Sci. USA 2007;104:961–966. [PubMed: 17215360]

(9). Lipinski MJ, Amirbekian V, Frias JC, Aguinaldo JG, Mani V, Briley-Saebo KC, Fuster V, Fallon JT, Fisher EA, Fayad ZA. MRI to detect atherosclerosis with gadolinium-containing immunomicelles targeting the macrophage scavenger receptor. Magn. Reson. Med 2006;56:601–610. [PubMed: 16902977]

(10). Ruehm SG, Corot C, Vogt P, Kolb S, Debatin JF. Magnetic resonance imaging of atherosclerotic plaque with ultrasmall superparamagnetic particles of iron oxide in hyperlipidemic rabbits. Circulation 2001;103:415–422. [PubMed: 11157694]

(11). Hyafil F, Cornily JC, Feig JE, Gordon R, Vucic E, Amirbekian V, Fisher EA, Fuster V, Feldman LJ, Fayad ZA. Noninvasive detection of macrophages using a nanoparticulate contrast agent for computed tomography. Nat. Med 2007;13:636–641. [PubMed: 17417649]

(12). Rudd JHF, Warburton EA, Fryer TD, Jones HA, Clark JC, Antoun N, Johnstrom P, Davenport AP, Kirkpatrick PJ, Arch BN, Pickard JD, Weissberg PL. Imaging atherosclerotic plaque inflammation with [F-18]-fluorodeoxyglucose positron emission tomography. Circulation 2002;105:2708–2711. [PubMed: 12057982]

(13). Nahrendorf M, Zhang H, Hembrador S, Panizzi P, Sosnovik DE, Aikawa E, Libby P, Swirski FK, Weissleder R. Nanoparticle PET-CT imaging of macrophages in inflammatory atherosclerosis. Circulation 2008;117:379–387. [PubMed: 18158358]

(14). Frias JC, Williams KJ, Fisher EA, Fayad ZA. Recombinant HDL-like nanoparticles: a specific contrast agent for MRI of atherosclerotic plaques. J. Am. Chem. Soc 2004;126:16316–16317. [PubMed: 15600321]

(15). Frias JC, Ma Y, Williams KJ, Fayad ZA, Fisher EA. Properties of a versatile nanoparticle platform contrast agent to image and characterize atherosclerotic plaques by magnetic resonance imaging. Nano Lett 2006;6:2220–2224. [PubMed: 17034087]

(16). Cormode DP, Briley-Saebo KC, Mulder WJM, Aguinaldo JGS, Barazza A, Ma Y, Fisher EA, Fayad ZA. An apoA-I mimetic peptide HDL-based MRI contrast agent for atherosclerotic plaque composition detection. Small 2008;4:1437–1444. [PubMed: 18712752]

(17). Anantharamaiah GM, Jones JL, Brouillette CG, Schmidt CF, Chung BH, Hughes TA, Bhown AS, Segrest JP. Studies of synthetic peptide analogs of the amphipathic helix. J. Biol. Chem 1985;260:10248–10255. [PubMed: 4019510]

(18). Tang C, Vaughan AM, Anantharamaiah GM, Oram JF. Janus kinase 2 modulates the lipid-removing but not protein-stabilizing interactions of amphipathic helices with ABCA1. J. Lipid Res 2006;47:107–114. [PubMed: 16210729]

(19). Anantharamaiah GM, Datta G, Garber DW. Toward the design of peptide mimics of antiatherogenic apolipoproteins A-I and E. Curr. Sci 2001;81:53–65.

(20). Navab M, Anantharamaiah GM, Reddy ST, Fogelman AM. Apolipoprotein A-I mimetic peptides and their role in atherosclerosis prevention. Nat. Clin. Pract., Cardiovasc. Med 2006;3:540–547. [PubMed: 16990839]

(21). Marque V, Kieffer P, Gayraud B, Lartaud-Idjouadiene I, Ramirez F, Atkinson J. Aortic wall mechanics and composition in a transgenic mouse model of Marfan syndrome. Arterioscler. Thromb. Vasc. Biol 2001;21:1184–1189. [PubMed: 11451749]

(22). Davidson WS, Lund-Katz S, Johnson WJ, Anantharamaiah GM, Palgunachari MN, Segrest JP, Rothblat GH, Phillips MC. The influence of apolipoprotein structure on the efflux of cellular free cholesterol to high density lipoprotein. J. Biol. Chem 1994;269:22975–22982. [PubMed: 8083197]

(23). Sosnovik D, Weissleder R. Magnetic resonance and fluorescence based molecular imaging technologies. Progress Drug Res 2005;62:86–114.

(24). Bocharov AV, Baranova IN, Vishnyakova TG, Remaley AT, Csako G, Thomas F, Patterson AP, Eggerman TL. Targeting of scavenger receptor class B type I by synthetic amphipathic α-helical-containing peptides blocks lipopolysaccharide (LPS) uptake and LPS-induced pro-inflammatory cytokine responses in THP-1 monocyte cells. J. Biol. Chem 2004;279:36072–36082. [PubMed: 15199068]

(25). Cormode DP, Skajaa T, van Schooneveld MM, Koole R, Jarzyna P, Lobatto ME, Calcagno C, Barazza A, Gordon RE, Zanzonico P, Fisher EA, Fayad ZA, Mulder WJM. Nanocrystal core high-density lipoproteins: A multimodal molecular imaging contrast agent platform. Nano Lett 2008;8:3715–3723. [PubMed: 18939808]

(26). Liu JB, Zeng FQ, Allen C. In vivo fate of unimers and micelles of a poly(ethylene glycol)-block-poly(caprolactone) copolymer in mice following intravenous administration. Eur. J. Pharm. Biopharm 2007;65:309–319. [PubMed: 17257817]

(27). Hoffman JS, Benditt EP. Plasma-clearance kinetics of the amyloid-related high density lipoprotein apoprotein, serum amyloid protein (ApoSAA), in the mouse - evidence for rapid ApoSAA clearance. J. Clin. Invest 1983;71:926–934. [PubMed: 6833494]

(28). Zahr AS, Davis CA, Pishko MV. Macrophage uptake of core-shell nanoparticles surface modified with poly(ethylene glycol). Langmuir 2006;22:8178–8185. [PubMed: 16952259]

(29). Kelly KA, Allport JR, Tsourkas A, Shinde-Patil VR, Josephson L, Weissleder R. Detection of vascular adhesion molecule-1 expression using a novel multimodal nanoparticle. Circ. Res 2005;96:327–336. [PubMed: 15653572]

(30). Nikanjam M, Blakely EA, Bjornstad KA, Shu X, Budinger TF, Forte TM. Synthetic nano-low density lipoprotein as targeted drug delivery vehicle for glioblastoma multiforme. Int. J. Pharm 2006;328:86–94. [PubMed: 16959446]

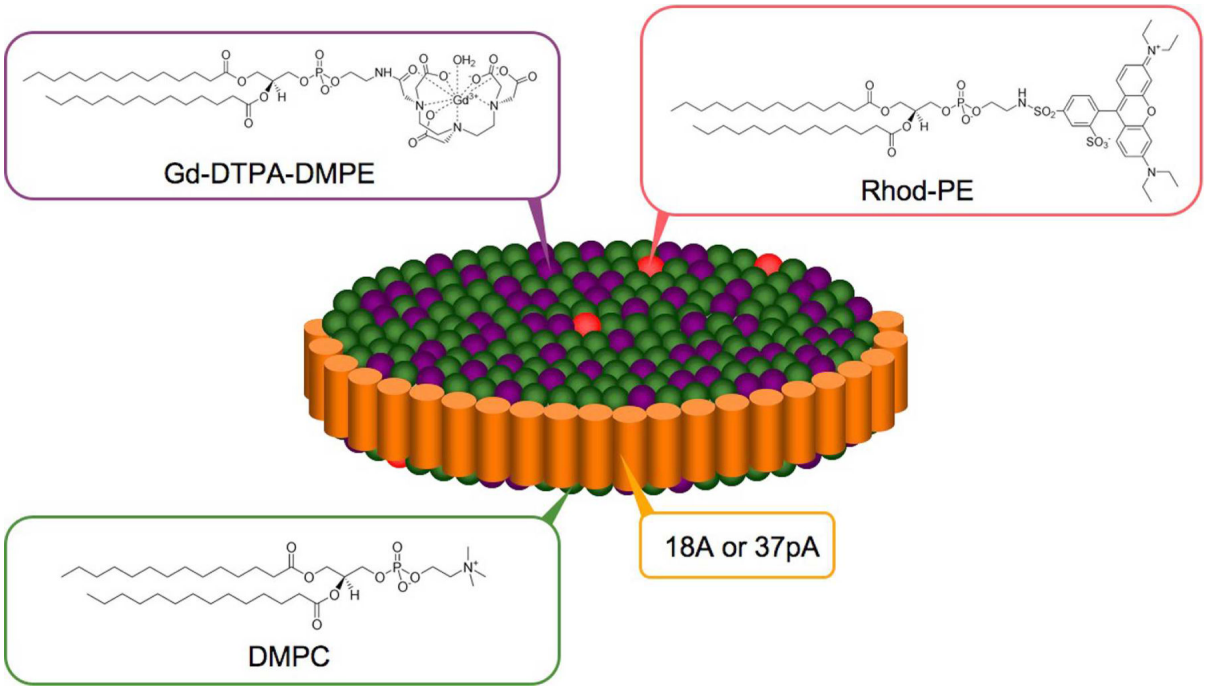

Figure 1.
Schematic depiction of the agents used in this study. DMPC is dimyristoyl phosphatidylcholine, Gd-DTPA-DMPE is gadolinium 1,2-dimyristoyl-sn-glycero-3-phosphoethanolamine diethylenetriamine pentaacetic acid and Rhod-PE is 1,2-dimyristoyl-sn-glycero-3-phosphoethanolamine-N-(lissamine rhodamine B sulfonyl) ammonium salt.

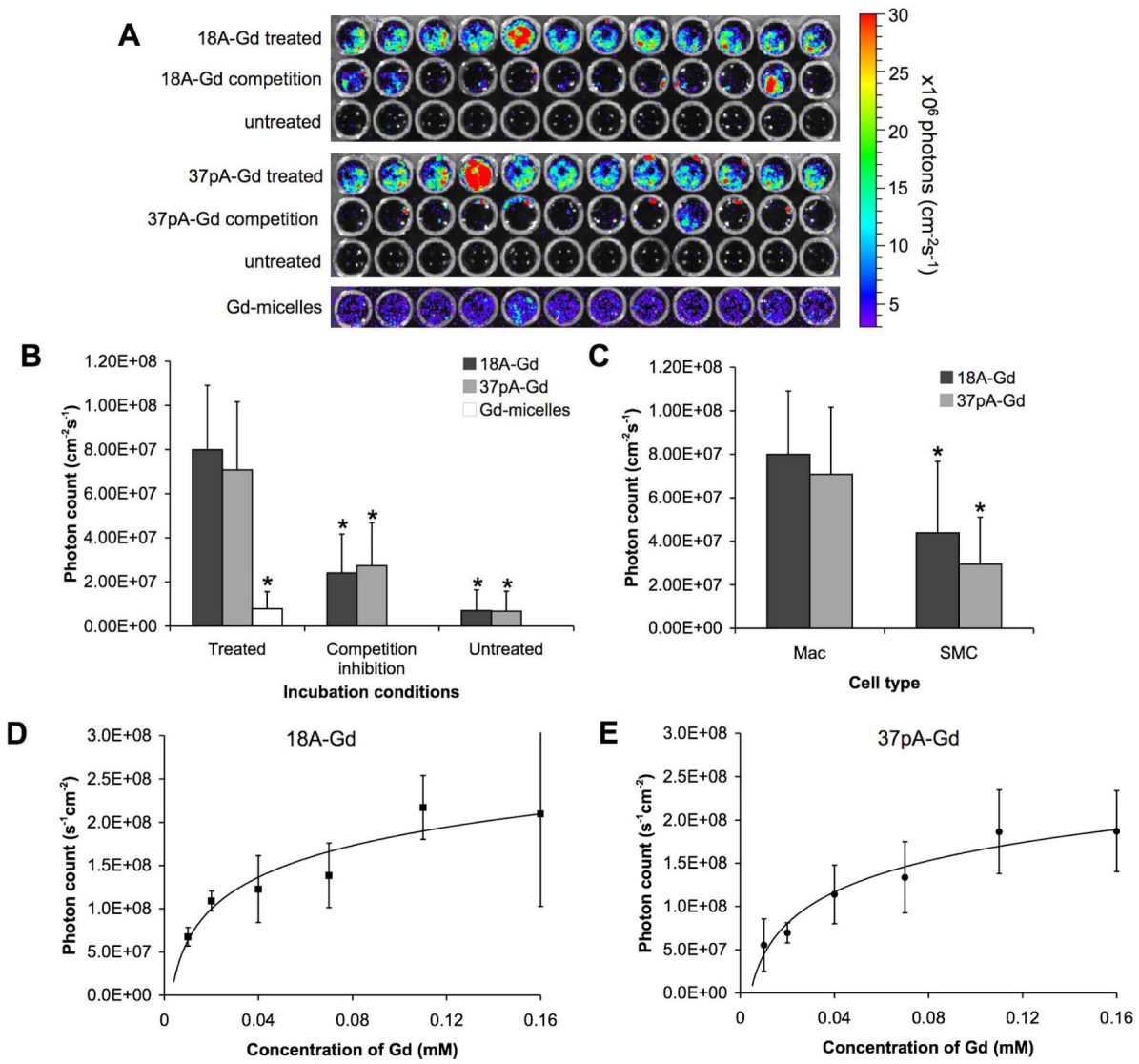

Figure 2.

In vitro uptake of Cy5.5 labeled synthetic HDL agents in J774A.1 murine macrophages. Uptake was assessed using an IVIS 200 fluorescent imaging system. A) Fluorescent images of cells treated with 18A-Gd or 37pA-Gd, with 18A-Gd or 37pA-Gd and a tenfold excess of agent without Cy5.5, untreated cells or treated with Gd-micelles. B) Quantified fluorescence of macrophages compared with macrophages under competition-inhibition conditions and untreated macrophages. Incubation conditions were 2 hours and 0.02 mM (by Gd) of agent. * indicates $p<0.01$ as compared to the treated macrophage cells. C) Comparison of the uptake of 18A-Gd and 37pA-Gd in macrophages and smooth muscle cells. D) and E) show the quantified fluorescence of 18A-Gd and 37pA-Gd respectively, when incubated for 2 hours at the indicated concentrations (the solid lines are logarithmic lines of best fit generated by a Matlab program). Error bars are equal to one standard deviation and n=12 in all cases.

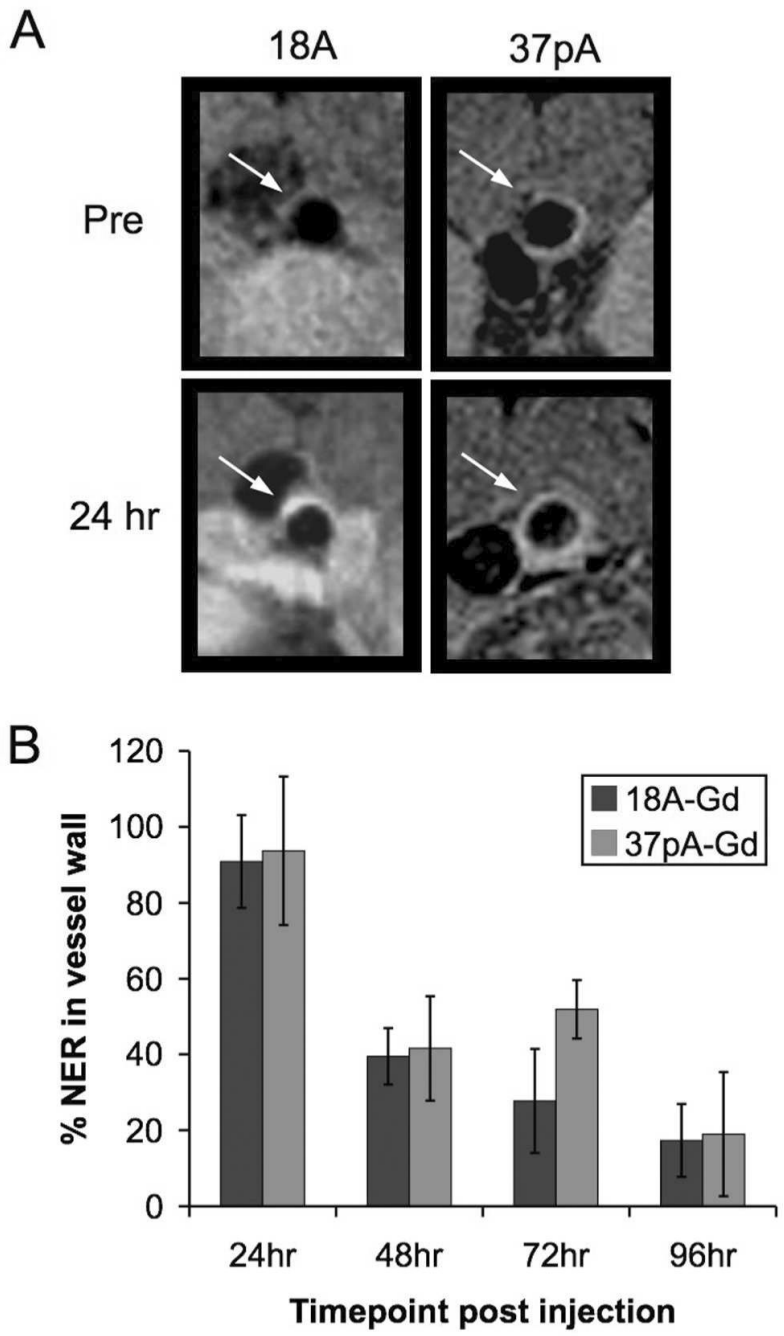

Figure 3.

A) Representative MR images of the aorta of apoE-KO mice pre- and 24 hours post-injection with 18A-Gd (left panels) and 37pA-Gd (right panels). B) Summary of the mean normalized enhancement ratio (% NER) at 24, 48, 72 and 96 hours in the aorta walls of apoE-KO mice injected with 18A-Gd or 37pA-Gd. Error bars are one standard deviation.

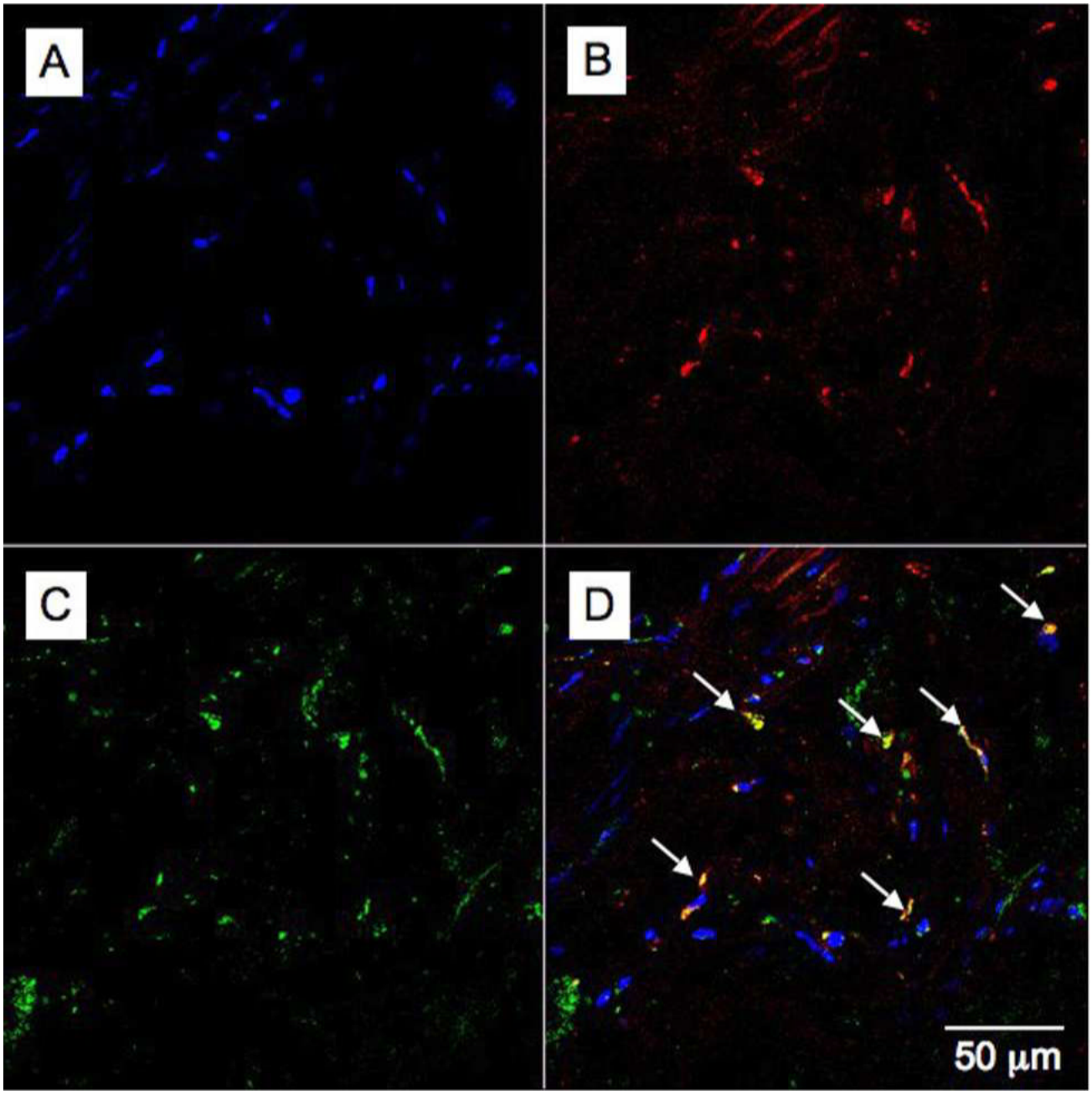

Figure 4.
Confocal microscopy images of aortic tissue excised from an apoE-KO mouse injected with the 18A-Gd agent 24 hours prior to excision. A - DAPI staining for nuclei (blue), B - the rhodamine channel (red) indicating areas of 18A-Gd uptake, C - Alexa 647:CD68 staining for macrophages (green) and D - merging the previous 3 images reveals the affinity of agent 18A-Gd for macrophages (yellow).

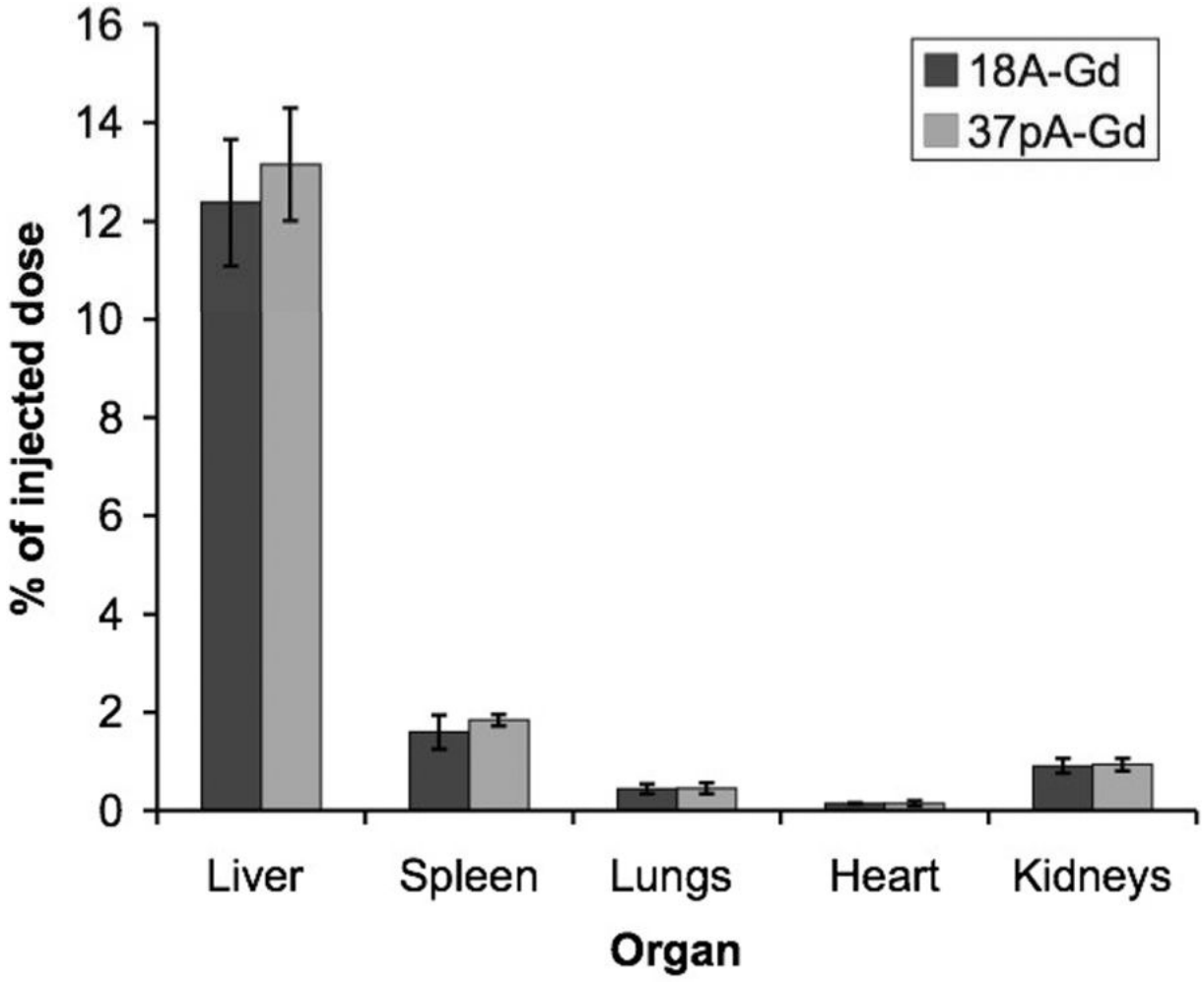

Figure 5.
Biodistribution of 18A-Gd and 37pA-Gd between the liver, spleen, lungs, heart and kidneys at 48 hours given as the percentage of the injected dose. Error bars are equal to one standard deviation and n=3 in each case.